NASA CR 114429
Available to the Public

Analysis Report Volume II

SILICON SOLAR CELL DEVELOPMENT AND RADIATION EFFECTS STUDY FOR LOW TEMPERATURE AND LOW ILLUMINATION INTENSITY OPERATION

Contract NAS2-5516

Submitted by:

Allen R. Kirkpatrick

Submitted to:

National Aeronautics and Space Administration
Ames Research Center
Moffett Field, California

Technical Monitor: R. J. Debs

January 1972

ION PHYSICS CORPORATION
IPC
A Subsidiary of High Voltage Engineering Corporation
BURLINGTON, MASSACHUSETTS

Analysis Report Volume II

SILICON SOLAR CELL DEVELOPMENT AND RADIATION EFFECTS STUDY FOR LOW TEMPERATURE AND LOW ILLUMINATION INTENSITY OPERATION

Allen R. Kirkpatrick

National Aeronautics and Space Administration
Ames Research Center
Moffett Field, California

Technical Monitor: R. J. Debs

Contract NAS2-5516

ION PHYSICS CORPORATION
BURLINGTON, MASSACHUSETTS

TABLE OF CONTENTS

LIST OF ILLUSTRATIONS

SECTION 1
INTRODUCTION AND SUMMARY

Volume I[1] of this Analysis Report described investigations performed to identify and analyze the mechanisms responsible for anomalous performance effects observed in silicon solar cells at low temperatures under low illumination intensities. Performance deficiencies were categorized, mechanisms involved were explained and necessary corrective steps in fabrication were outlined.

This Volume II of the Analysis Report describes completion of the examination of performance problems and presents the results of a study to determine the effect of in-situ proton irradiation upon low temperature, low intensity performance of several cell types. Included in this report are recommendations for an optimized cell for Jupiter probe use and definition of the testing required on these cells to insure good performance characteristics.

Five cell types were included in the in-situ 1 MeV proton irradiation study. These types were selected in an attempt to distinguish variations in temperature-dependent radiation resistance which could be attributed to the N/P or P/N structure, diffused or implanted junctions, crucible grown or float-zone type base material and high or low base resistivity. While expected variations in performance were observed at room temperature, all cell types degraded more or less similarly at lower temperatures with normalized degradation becoming increasingly rapid as temperature was reduced. A number of annealing effects were observed but it is evident that any solar cell operating at low temperature will be extremely vulnerable to radiation-induced degradation.

The rapid degradation of cell output at low temperatures due to proton damage demands that cells be particularly well shielded against any proton environment associated with a low temperature mission. In the case of a Jupiter probe there exists a strong possibility that high fluences of trapped protons with energies in the range 5 to 50 MeV will be encountered. Solar cells to be used on such a mission should be shielded against as much of this environment as

possible. A small area panel with exceptionally thick coverglass protection used in conjunction with solar concentrators could be advantageous.

SECTION 2

SUMMARY OF LOW TEMPERATURE/LOW INTENSITY EFFECTS

2.1 Performance Problems

Classification and explanation of problems associated with solar cell low temperature/low intensity operation have been discussed at length in Volume I[1] of this Analysis Report. In brief, it is possible to identify cell operation at low temperature and intensity as falling into one of four categories illustrated in Figure 1. Another operational group has been reported elsewhere[2] as including cells which experience excessive I_{sc} decrease as temperature is reduced. The performance categories of Figure 1 include:

(1) 'ideal' high performance
(2) rectifying contact problem
(3) low shunt resistance problem
(4) 'double slope' edge conduction problem

Incidence of the operational problems is strongly dependent upon cell fabrication procedures. Consequently the distribution of cells among the good and problem categories has varied widely among conventional cells from different manufacturers. Observed behavior can be explained in terms of an equivalent circuit derived from a simple model of the solar cell structure.

Equivalent circuit elements which must be considered in association with the cell junction are shown in Figure 2. The cell is separated into body and edge regions. The body consists of the p-n junction, a junction defect shunt resistance in parallel with the junction and possibly a Schottky barrier in series with the junction at the back contact. The back contact Schottky barrier will not be present if precautions are taken during fabrication to assure its absence. The cell edge consists of a resistive element in series with a rectifying element. More than one explanation for this edge model is possible. IPC believes that the resistive element is formed by a thin inversion or accumulation

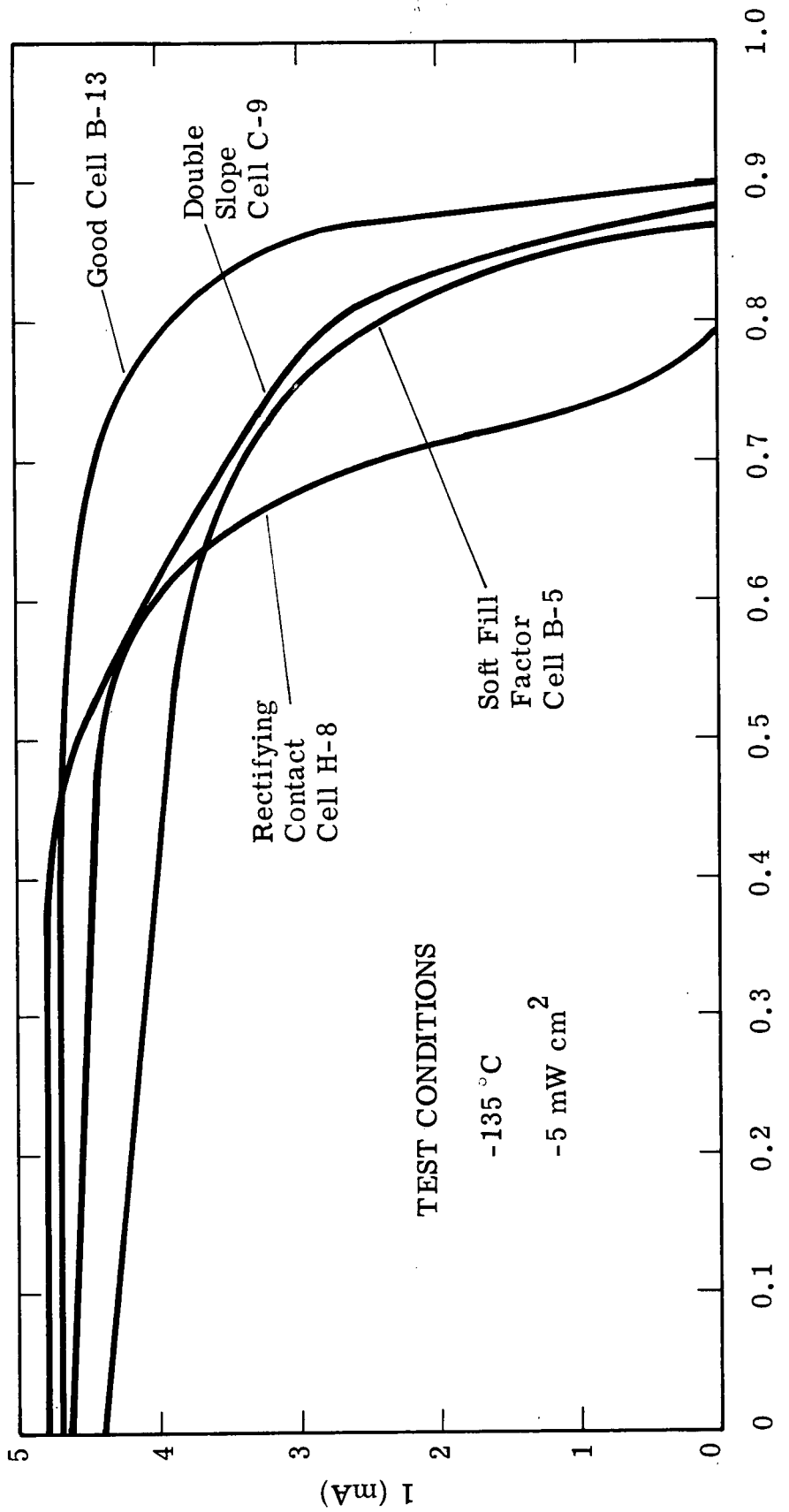

Figure 1. Typical Low Temperature, Low Intensity Solar Cell Output Characteristics.

1-6359

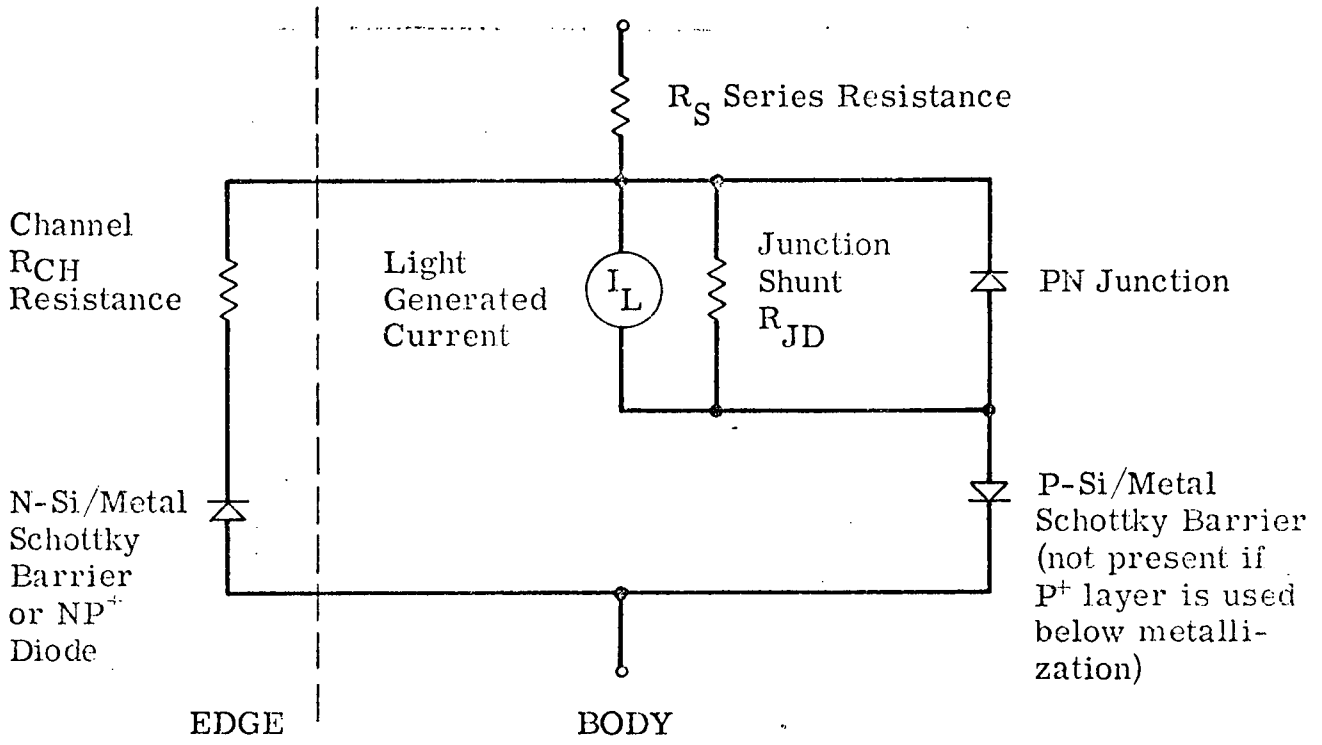

Figure 2. Equivalent Circuit of the N/P Solar Cell.

1-5092

layer channel on the silicon surface, and the junction or Schottky barrier diode resides at the interface between this channel and opposite type silicon or contact metallization. The mechanisms involved have been described in detail in Volume I of this report and in reference 3.

A cell exhibiting the characteristic rectifying contact problem behavior at low temperature is one in which a Schottky barrier is present in the body branch of the cell equivalent circuit at the back contact. The Schottky barriers which is produced at the interface between lightly doped base region silicon and the contact metals is forward biased when the cell is illuminated. Cell output voltage is lost in order to forward bias the barrier to conduct cell current. The barrier can be eliminated by introducing a heavily-doped layer into the silicon below the back contact by alloying or diffusion.

Directly across the cell junction is a shunt path with resistance which is determined by the presence of junction defects. In a typical good cell this resistance is very high and is of no consequence to cell performance even under illumination intensities of only a few milliwatts per cm^2. However, damaged junction structures can be fabricated in which the junction shunt resistance is sufficiently low to cause poor fill factors under low intensity operation. Generally this will occur because of penetration of the front contact metallization through the junction, probably in the form of localized filamentary paths. The problem can best be avoided by producing uniformly deep junctions not locally shallower than 0.25μ over the cell surface.

The presence of a conducting channel down the edge of the cell is of considerable importance to the low temperature, low intensity cell operation. A diode element occurs in series with the edge channel. In the case of the N/P cell with N-type surface inversion layer, the rectifying element is formed at the interface of the channel layer and the back contact metallization (or the heavily doped P^+ layer sometimes introduced under the contact). The edge channel diode is always biased in the same direction as the cell junction. At room temperature negligible voltage is required to pass forward current across this diode and the edge component of the structure appears simply as a contribution to shunt resistance. At lower temperatures up to several hundred millivolts

may be required to turn-on the edge diode. At output voltages below that producing diode turn-on, the diode blocks current through the edge channel. When turn-on occurs, the edge channel appears as a conductive shunt between the cell front and back contacts. If resistance of the edge channel is sufficiently low, the 'double slope' problem output characteristic results.

Assured elimination of the excessive edge conduction problem would require major modification to existing conventional cell structure. Such modification could, for example, involve use of a planar geometry without exposed junction at the cell edge. However IPC has observed only occasional incidence of the double slope problem in cells sized by scribing after contacts and anti-reflective coatings have been applied. Also it has been found that an etched edge cell exhibiting the double slope problem can generally be improved by re-etching its edges in a 6-1-1 (parts HF, HNO_3, HAc) solution. Use of a scribed edge cell and simplified dark liquid nitrogen submersion testing described in Section 5 should adequately avoid the double slope performance deficiency.

SECTION 3
IRRADIATION STUDIES

3.1 Introduction

In order to define a cell design optimized for operation at low temperature and intensity on a mission which could also include simultaneous encounter with a significant radiation environment, some knowledge of degradation effects to be involved is required. At present in the absence of flight data, it is not possible to anticipate with confidence the radiation threat which will be experienced by a probe to Jupiter. Predictions which have been made[4,5] of the Jovian environment suggest that the electron component will probably be of minor consequence compared to potential proton radiation exposure. The basis for this conclusion is that protons in any Jovian trapped radiation belts are predicted to be of sufficiently high energy to penetrate coverglass protection of any realistic thickness.

Existing experimental data related to solar cell irradiations at low temperatures indicate electron exposure effects[6] to be more, but not excessively more, serious at low temperature than at 28°C. On the other hand, proton irradiations at low temperatures[7] have resulted in much greater relative degradation than is observed at room temperature. Because of the importance of the proton environment and the apparent strong temperature dependence of proton degradation effects, it was decided to investigate proton degradation as a function of irradiation temperature for a number of silicon cell types. Exceptional resistance to proton degradation at low temperatures by specific cell types could be of considerable importance in the selection of an optimized solar cell for a Jupiter mission.

3.2 Experimental Study

A proton irradiation program was carried out on cells of five types described in Table I. Centralab cells were supplied by Dr. R. J. Debs of NASA

Ames Research Center. Cell leads, except those to the backs of the Centralab P/N and N/P cells, were 0.070" x 0.003" aluminum strip attached by ultrasonic welding. Unreliable welds were obtained on some of the Centralab cell backs and soldered silver strip was used instead. Redundant leads were used to allow separate monitoring of cell current and voltage. A common back lead was used for strings of three cells and the two ends of the lead served as the redundant connections.

Cells to be irradiated were mounted in groups of six on 0.250" thick copper plates which were fastened to a coolant reservoir. Each group included the five cell types of Table I. Slots in the plates accommodated the cell common back leads which were clamped to the plates at the external lead connection posts. A heated copper block used between the cell plate and reservoir allowed continuous variation over a wide temperature range but generally measurements were made only at 28 °C, -70 °C, -160 °C and -180 °C. Temperature was monitored using thermocouples attached to the cell plate. Irradiation series were performed at specific constant temperatures which were maintained without interruption throughout the irradiation and data accumulation sequences. Prior to irradiation and after the final irradiation step of a series, data was taken at other selected temperatures.

Irradiations were done using an IPC 2 MeV Van de Graaff accelerator. A beam of protons of 1 MeV energy was electrostatically scanned to uniformly irradiate a 5 x 8 cm area of the sample holder. The fluence was determined from the total charge carried by the beam to the sample holder. Since the mean range of 1 MeV protons in silicon is 16 micrometers, radiation damage was produced to a depth corresponding to about 50 times the junction depth. After each irradiation step the cell holder and reservoir could be rotated 180 ° away from the proton beam port to face illumination through a 6" diameter window. Illumination was provided by an ultrastable 3200 °K color temperature unfiltered tungsten-iodine source. Intensity over the cell holder was measured using an Eppley thermopile and was monitored during each data recording. Intensity varied by ±2% over the cell holder and remained stable to within ±1% during irradiation runs.

Table I. Cell Types in Irradiation Tests

Type	Manufacturer	Structure	Base Material	Nominal Thickness	Junction	Contacts	Antireflective Coating
1	IPC	N^+/PP^+	1Ω-cm Lopex	15 mils	Implanted	Ti/Ag**	CeO_2
2	IPC	N^+/PP^+	10Ω-cm Lopex	10 mils	Implanted	Ti/Ag**	CeO_2
3	IPC	N^+/PP^+	10Ω-cm Lopex	10 mils	Diffused	Aluminum**	SiO_x
4*	Centralab	N^+/P	10Ω-cm CG	15 mils	Diffused	Ti/Ag	SiO_x
5*	Centralab	P^+/N	10Ω-cm CG	15 mils	Diffused	Ti/Ag	SiO_x

*Cells supplied by R. J. Debs. Quartz crucible grown (CG) base material.
**Alloyed aluminum underlayer at cell back

3.3 Irradiation Test Data

3.3.1 In-Situ Irradiation and Measurement

The effect of a series of low temperature irradiations on the in-situ low temperature, low illumination intensity output I-V characteristics of a typical cell is illustrated in Figure 3a. The results of equivalent irradiations and measurements at 28 °C on a similar cell are shown for comparison in Figure 3b.

As cell operating temperature is decreased, irradiation causes more severe degradation of output current and with one exception has only moderate effect on V_{oc}. The exception can occur in the case of a cell with the double slope problem at low temperature and intensity. A rather extreme example is shown by cell 10 CG84-9 of Figure 4. In the case of a cell with less serious double slope deficiency, V_{oc} would degrade slowly with increasing irradiation as long as I_{sc} exceeded edge current at V_{oc}. When maximum edge current became essentially equal to I_{sc}, V_{oc} would become limited by the double slope portion of the I-V characteristic and would decrease rapidly with decreasing current.

Degradation of cell maximum power is primarily dependent upon loss of output current and consequently also becomes increasingly rapid as operating temperature is reduced. In Figure 5 normalized maximum power output for a particular cell type is given as a function of proton fluence for irradiation and measurement at 28 °C, -70 °C, -160 °C and -180 °C. The same trend is observed for all cell types investigated.

A series of irradiations and measurements in-situ at 28 °C, -70 °C, -160 °C and -180 °C were made in which cells utilized were screened using the procedures of Section 5 to eliminate those with bad initial performance at low temperature and intensity. Because limited numbers of diffused CG 10 ohm-cm N/P, implanted Lopex 1 ohm-cm N/P and diffused CG 10 ohm-cm P/N cells were available, it was in some cases necessary to utilize cells with low shunt resistance or minor double slope characteristics and eliminate only those with serious deficiencies. However, all cells for these runs exhibited at least moderately good output characteristics. Normalized low intensity I_{sc} versus

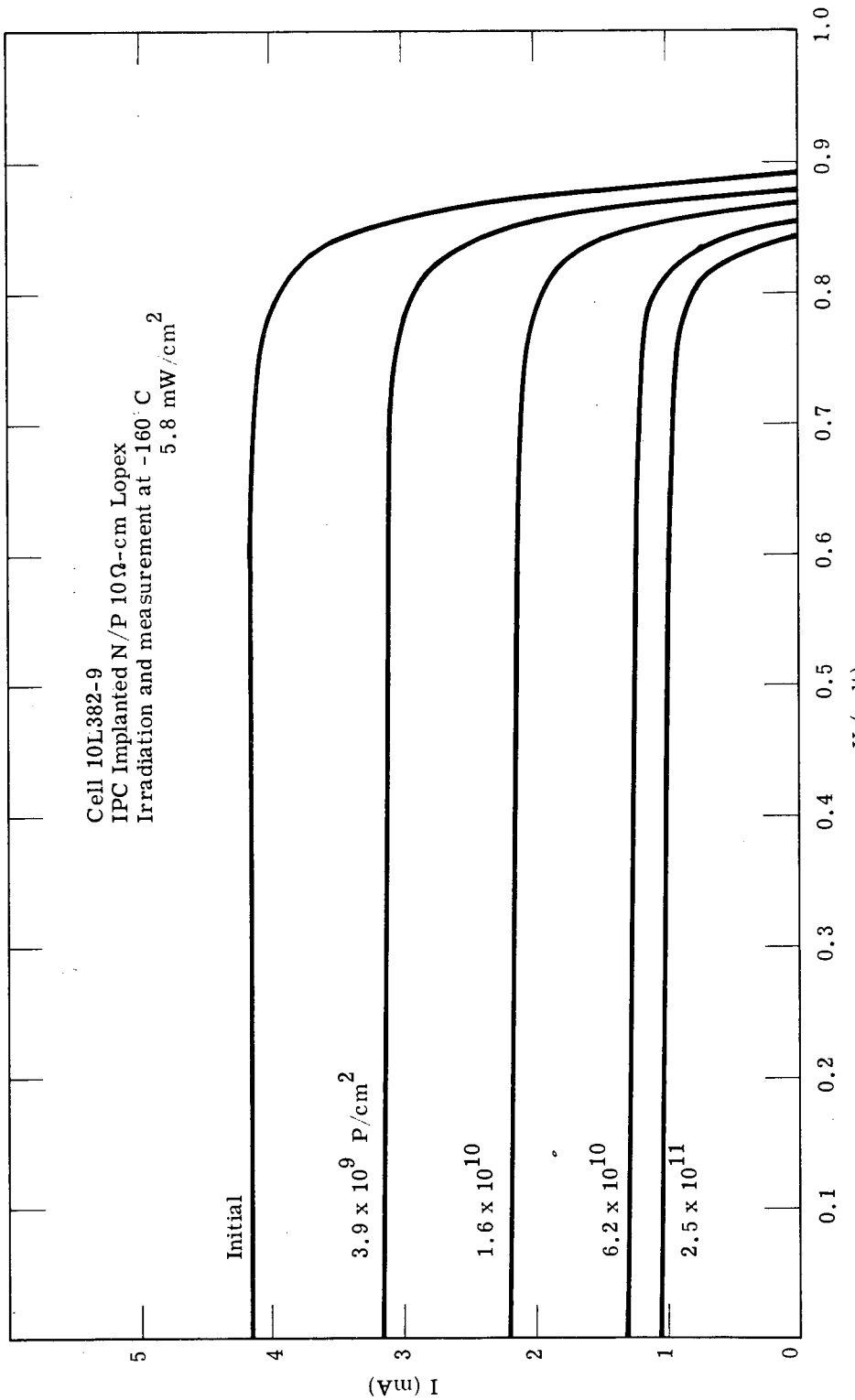

Figure 3a. Illuminated I-V Characteristics at -160 °C as Function of Irradiation Fluence.

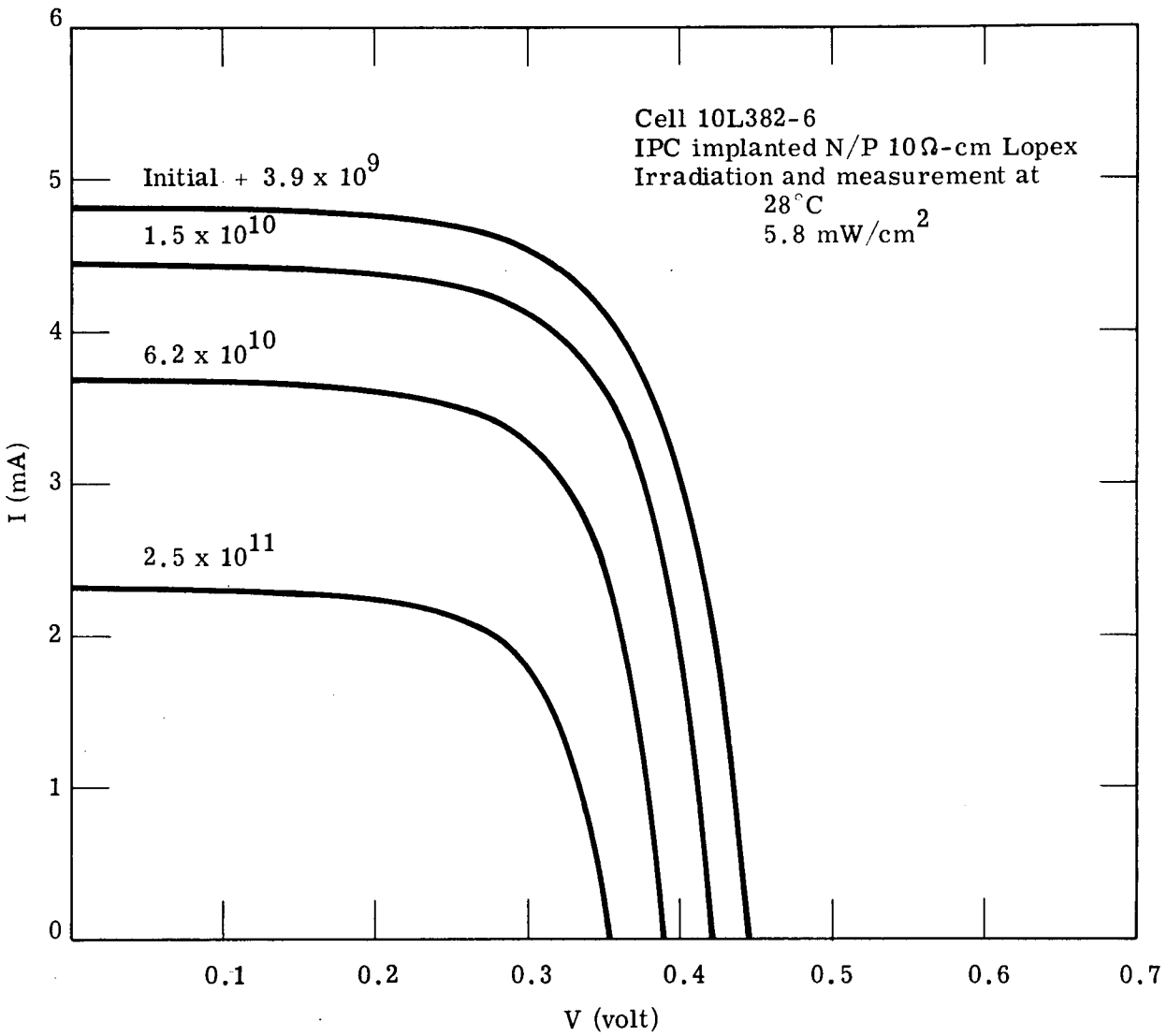

Figure 3b. Illuminated I-V Characteristics at 28 °C as Function of Irradiation Fluence.

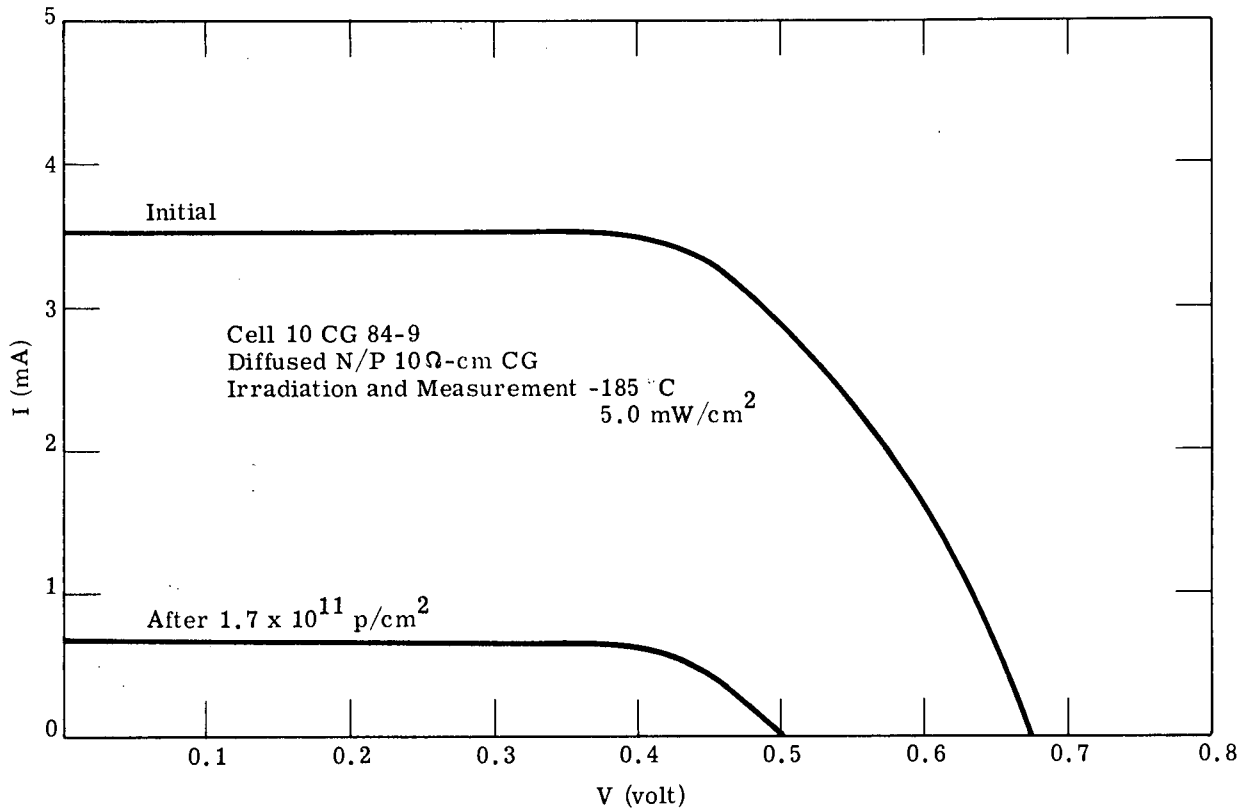

Figure 4. The Effect of Irradiation on a Cell with Excessive Edge Conduction.

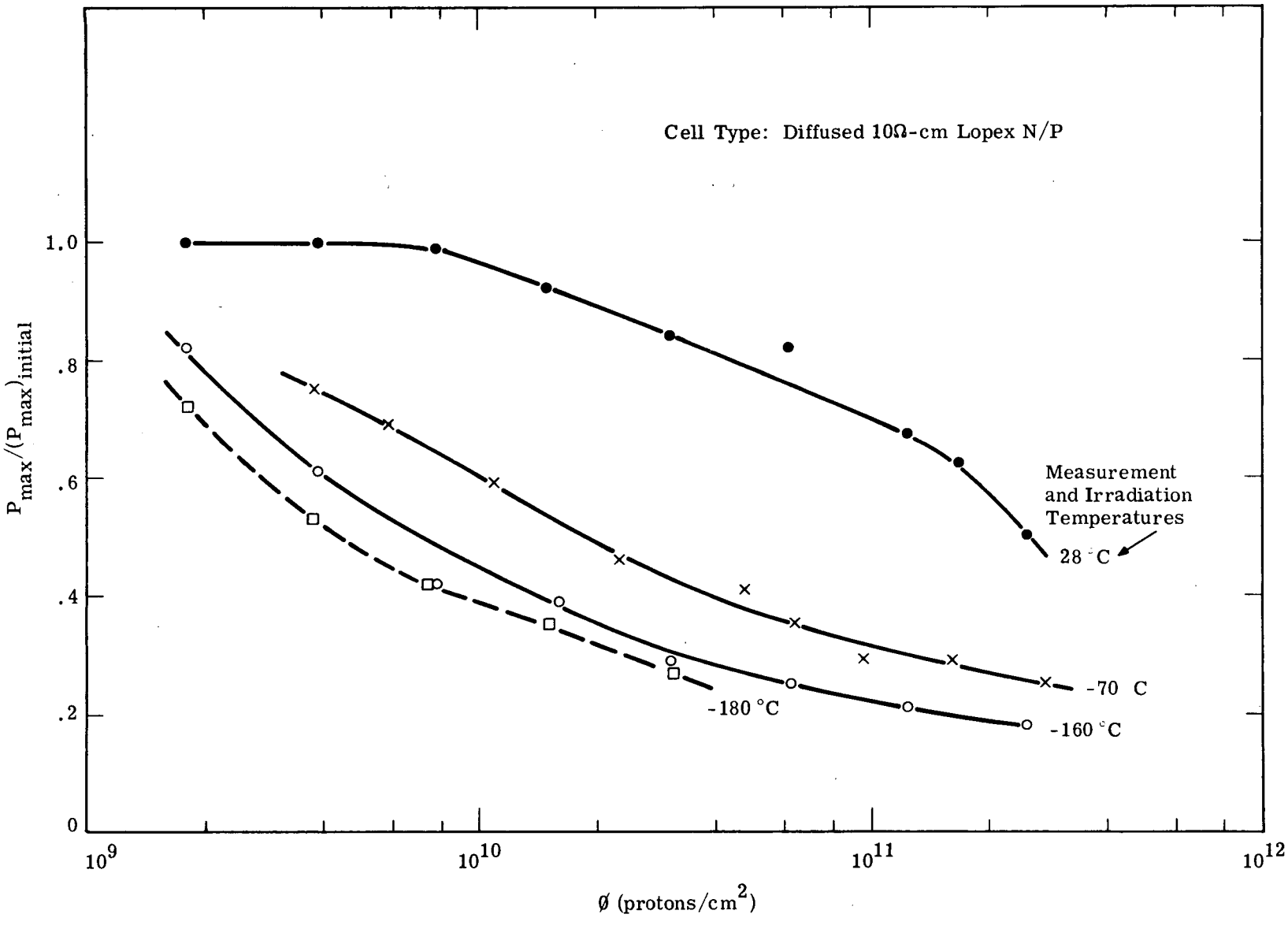

Figure 5. The Effect of Temperature on Degradation of P_{max}.

proton fluence curves for individual cells of each type are given in Figures 6, 7, 8 and 9 for irradiation and measurement temperatures of 28 °C, -70 °C, -160 °C and -180 °C respectively. Associated normalized P_{max} curves for the same cells are shown in Figures 10 through 13. It is apparent from inspection of these curves that while there exists a wide variation in sensitivity of the five cell types to proton irradiation at room temperature, at -70 °C and below, all types exhibit similar, perhaps almost identical, degradation rates.

Fluences of 1 MeV protons to degrade cell I_{sc} and P_{max} by 25 and 50% at each irradiation and test temperature above are tabulated in Table II. These critical fluences are valid only for the unfiltered 3200 °K color temperature spectrum utilized in these tests. It can be seen that while critical fluences at 28 °C vary among cell types by an order of magnitude or more, at the lower temperatures the critical fluences agree to within a factor of approximately two or at most three.

3.3.2 Performance at Temperatures Other than that of Irradiation

The results described above apply to irradiations and characterization measurements made without change in cell temperature. It was also considered to be of some interest to observe the effect of irradiation at one temperature upon performance at another temperature. For this purpose data was taken for each cell at more than one temperature before each irradiation series and again after the final irradiation step.

Tabulated in Table III are fractions of initial P_{max} remaining at different temperatures after irradiation to 2.5×10^{11} protons cm^{-2} at 28 °C, -70 °C and -160 °C. These data are from the cells also represented in Figures 6 through 13. Similarities to the in-situ results can be noted: regardless of irradiation temperature, fractional performance loss is greatest at the lowest operating temperature; differences between cell types is greatest when the irradiation or the measurement temperature was 28 °C.

From the limited data obtained, it is not possible to determine a correlation between the effects of identical irradiations at different temperatures upon performance at some fixed temperature. Clearly degree of

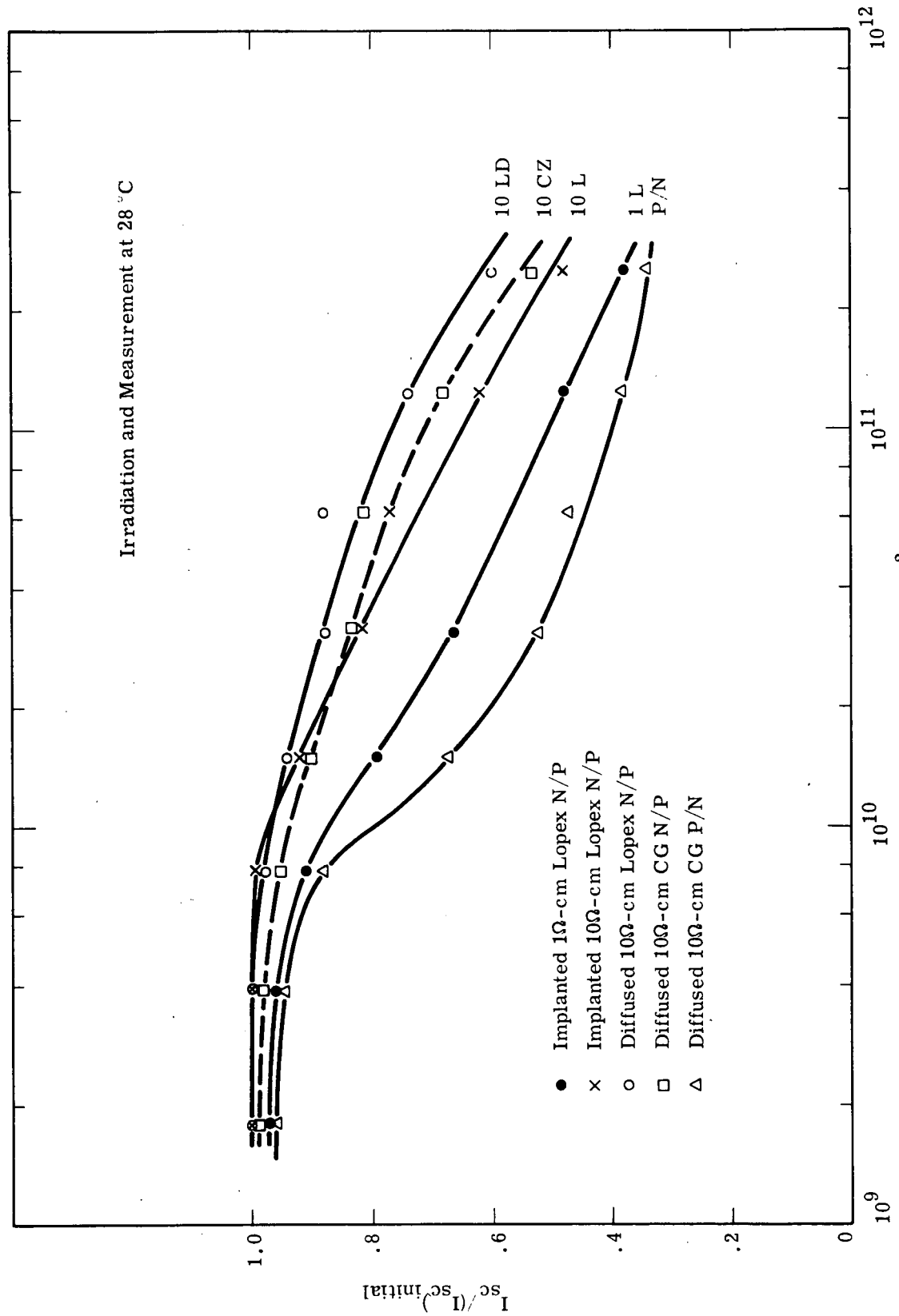

Figure 6. I_{sc} Degradation at 28 °C.

1-6322

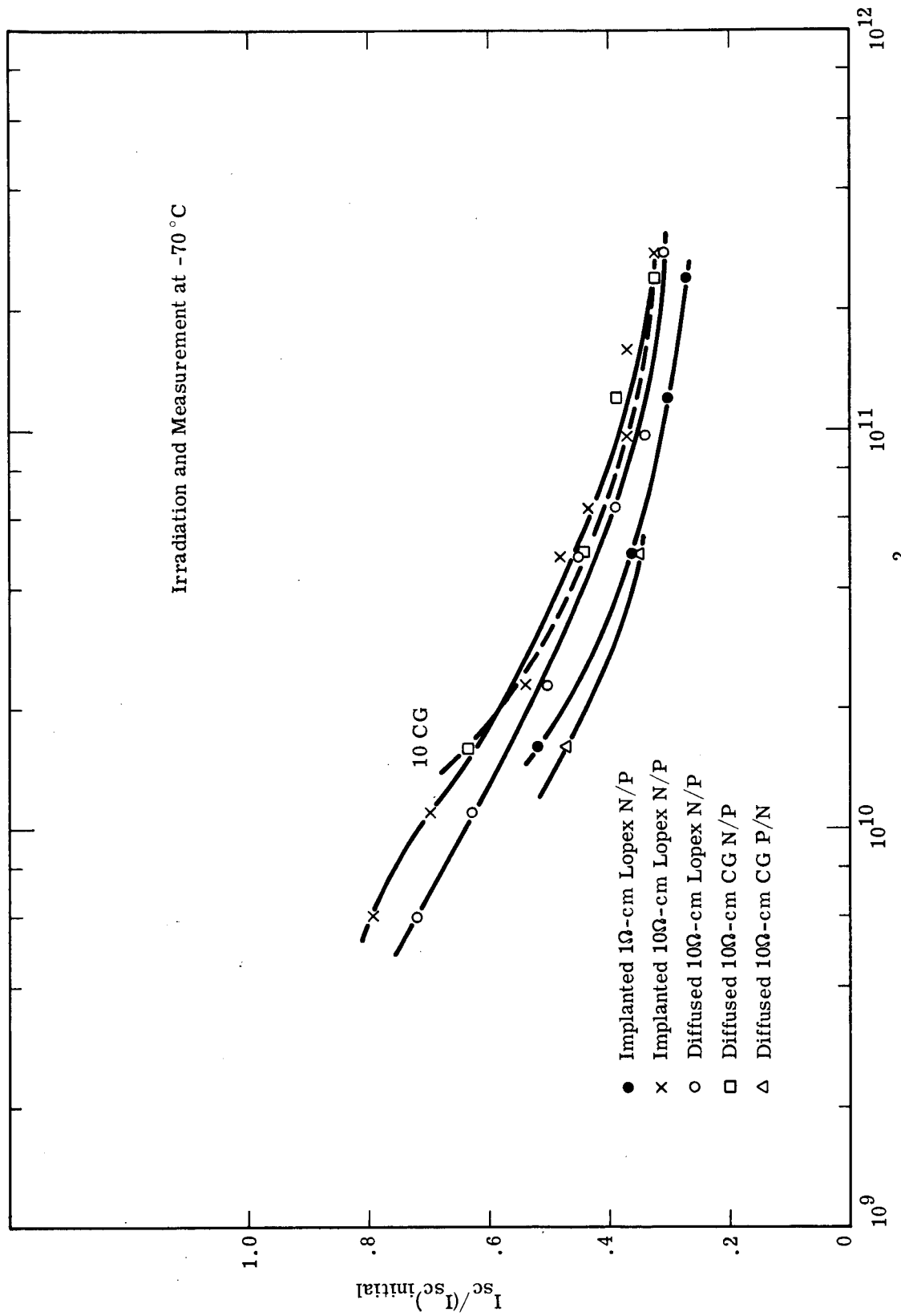

Figure 7. I_{sc} Degradation at -70 °C.

1-6323

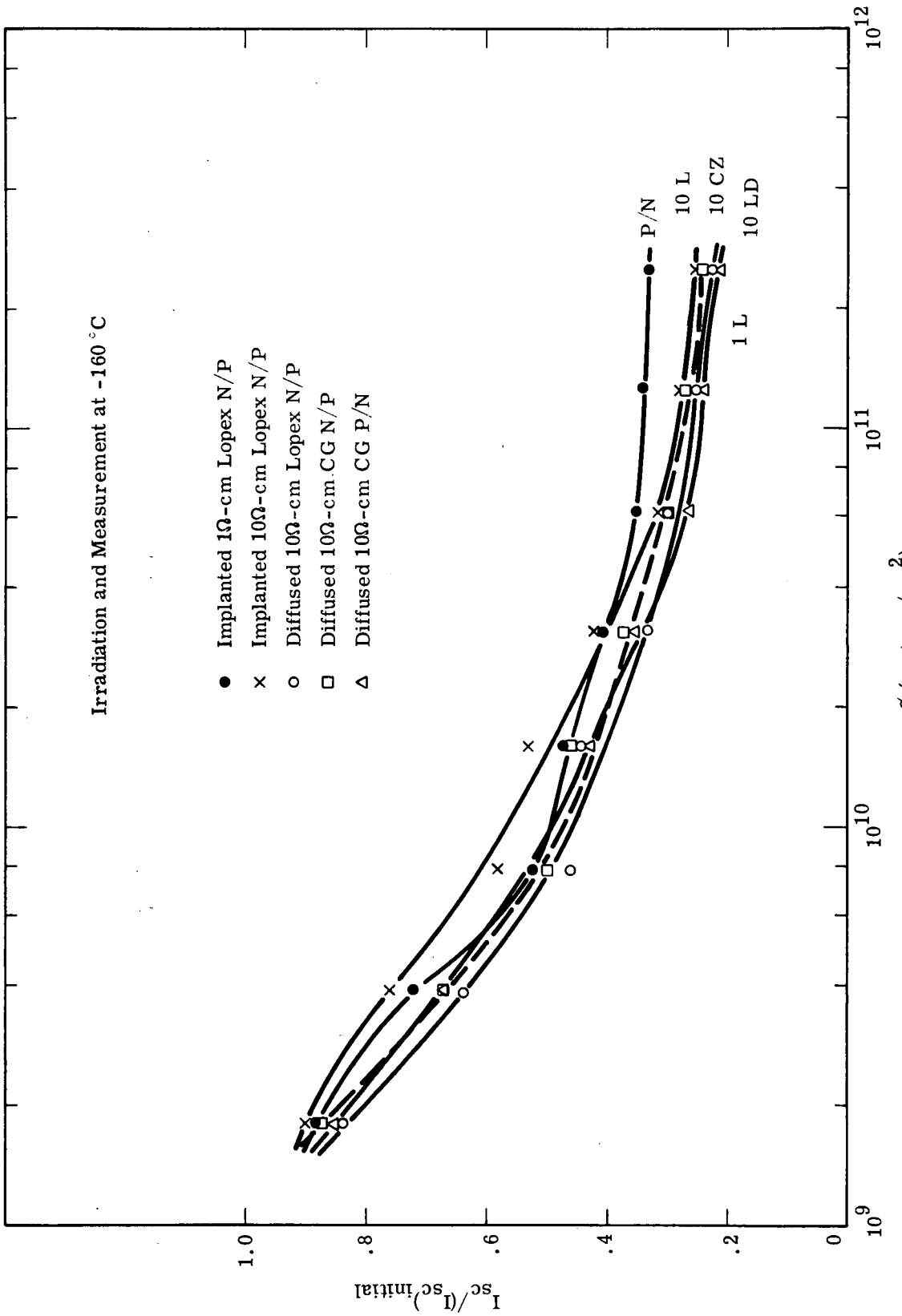

Figure 8. I_{sc} Degradation at -160 °C.

1-6324

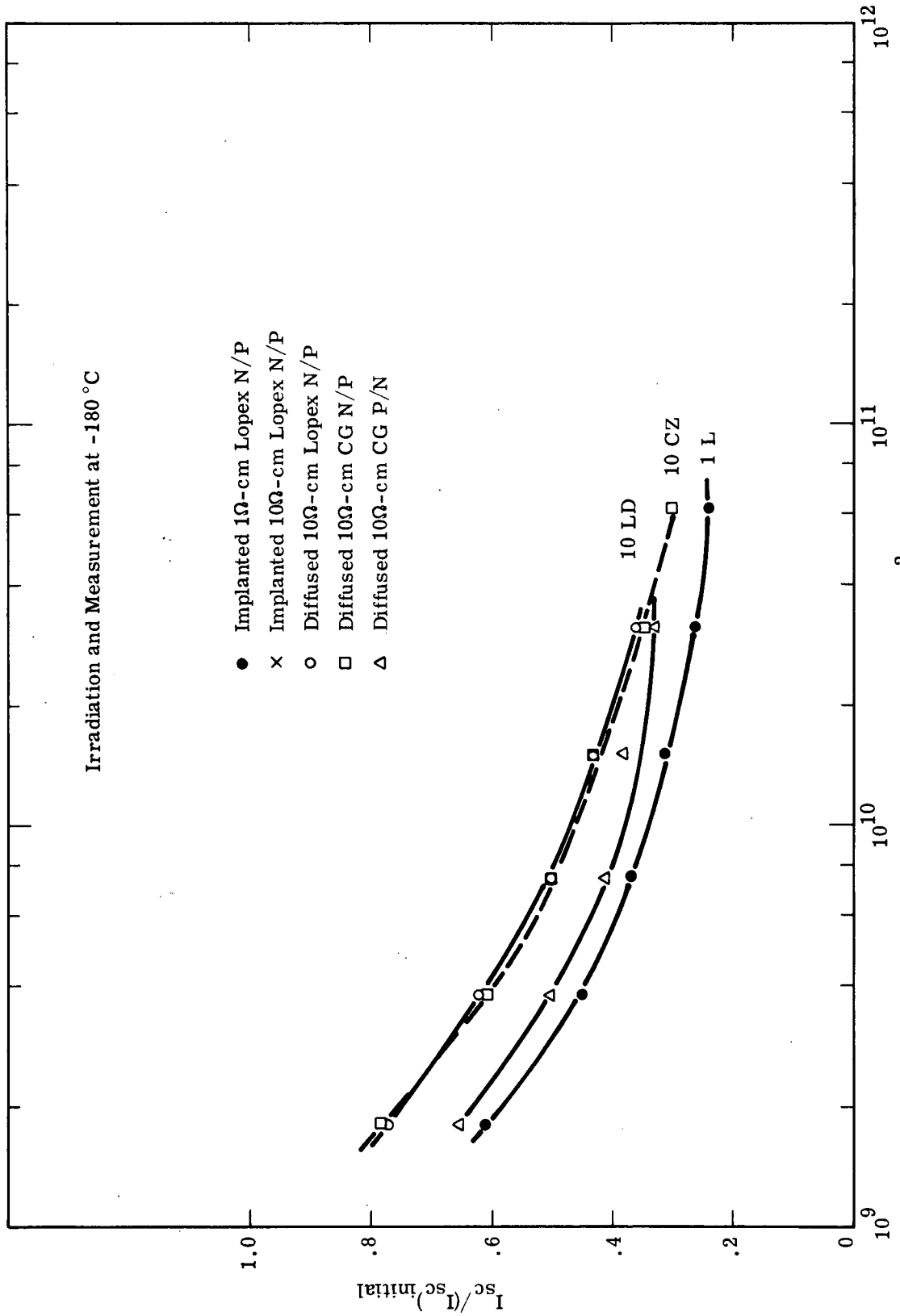

Figure 9. I_{sc} Degradation at -180 °C.

1-6325

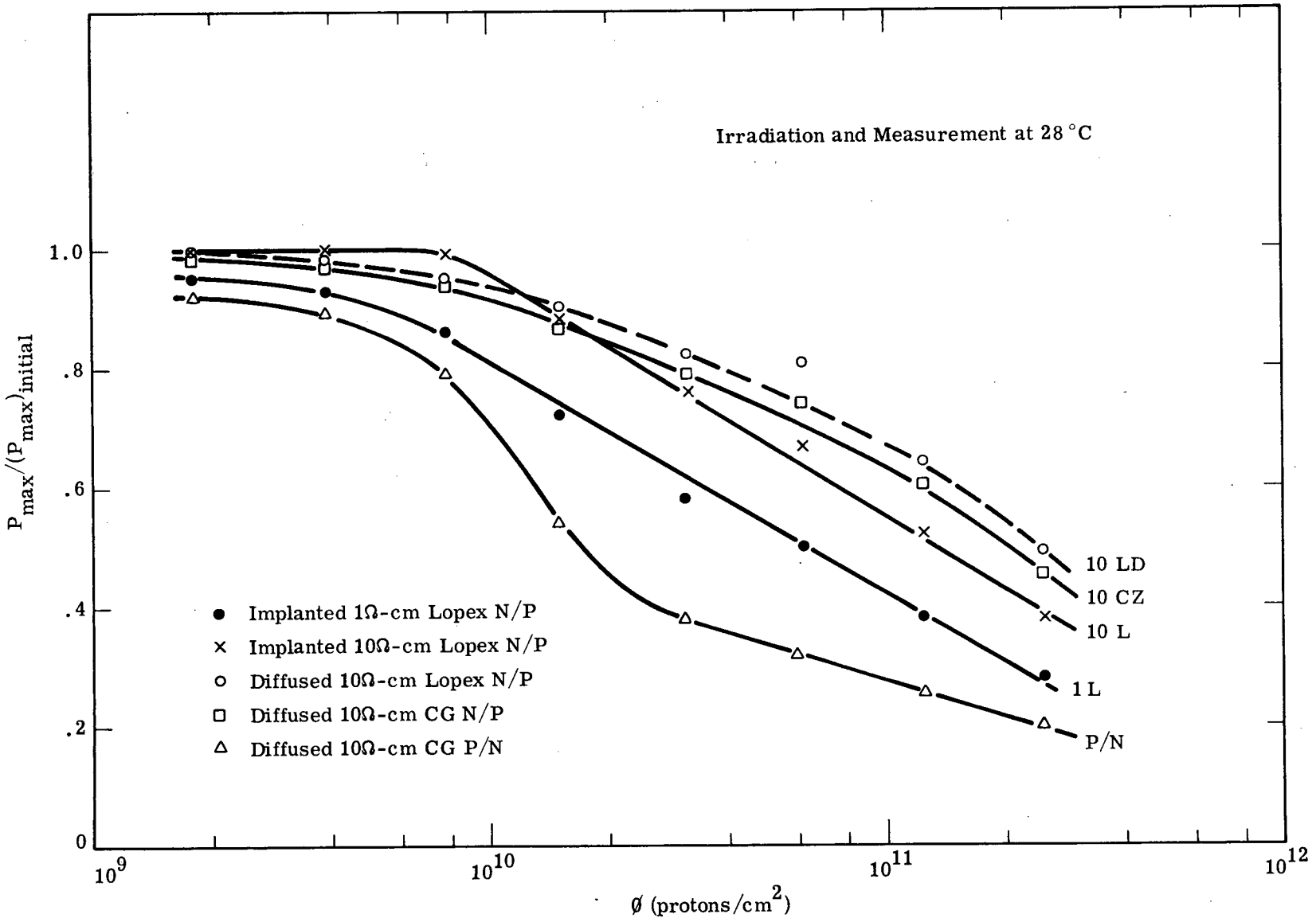

Figure 10. P_{max} Degradation at 28 °C.

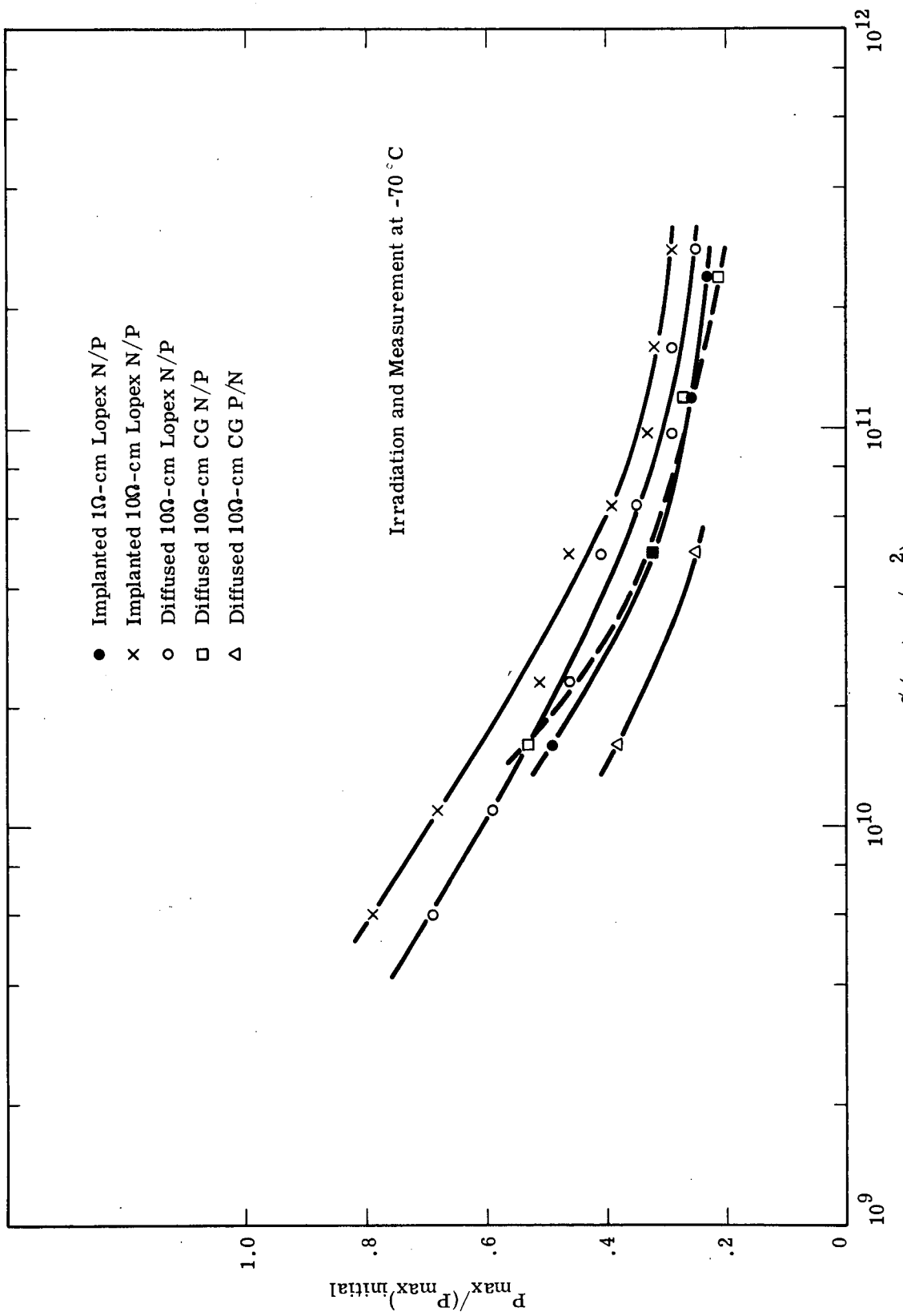

Figure 11. P_{max} Degradation at -70 °C.

1-6327

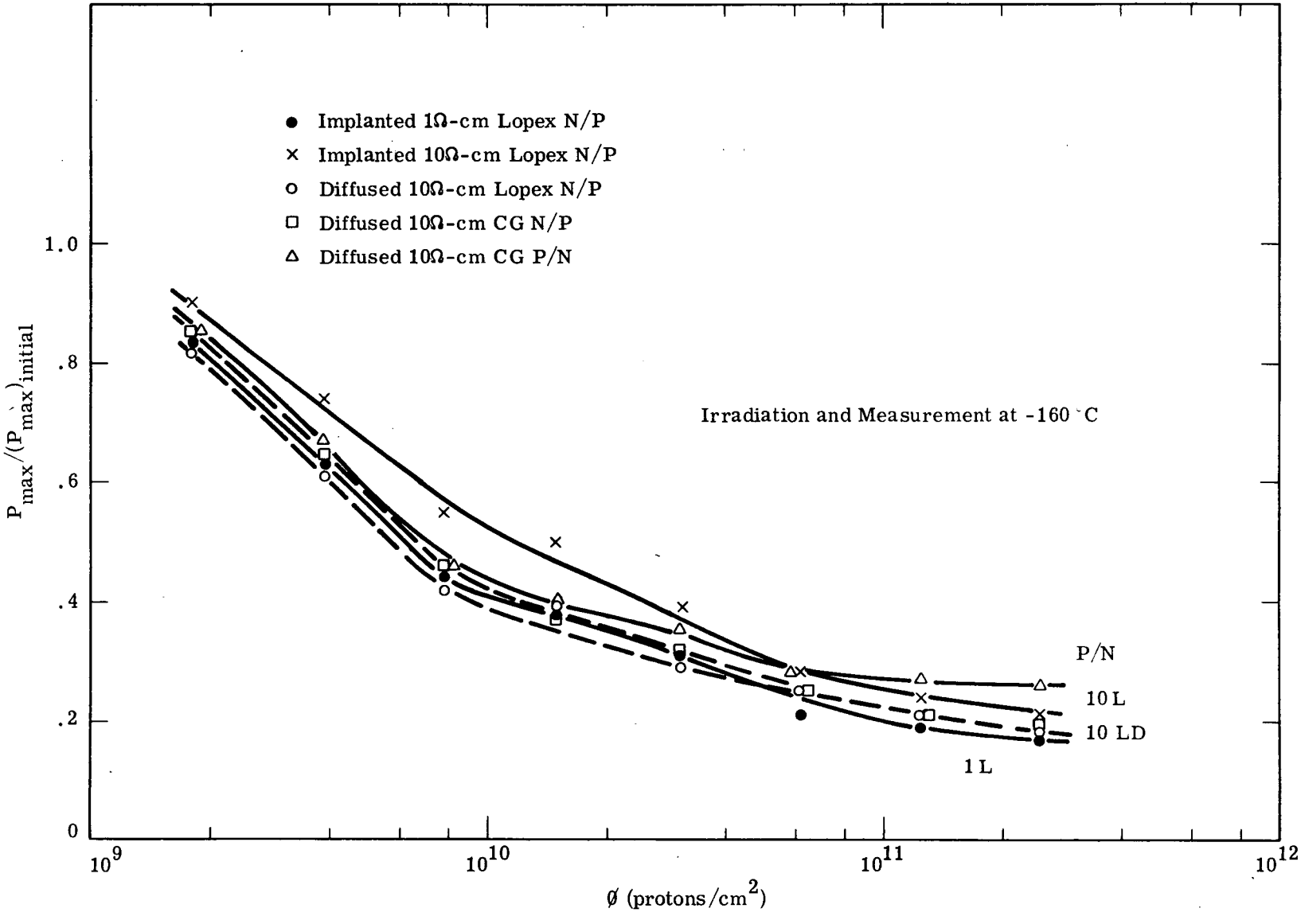

Figure 12. P_{max} Degradation at -160 °C.

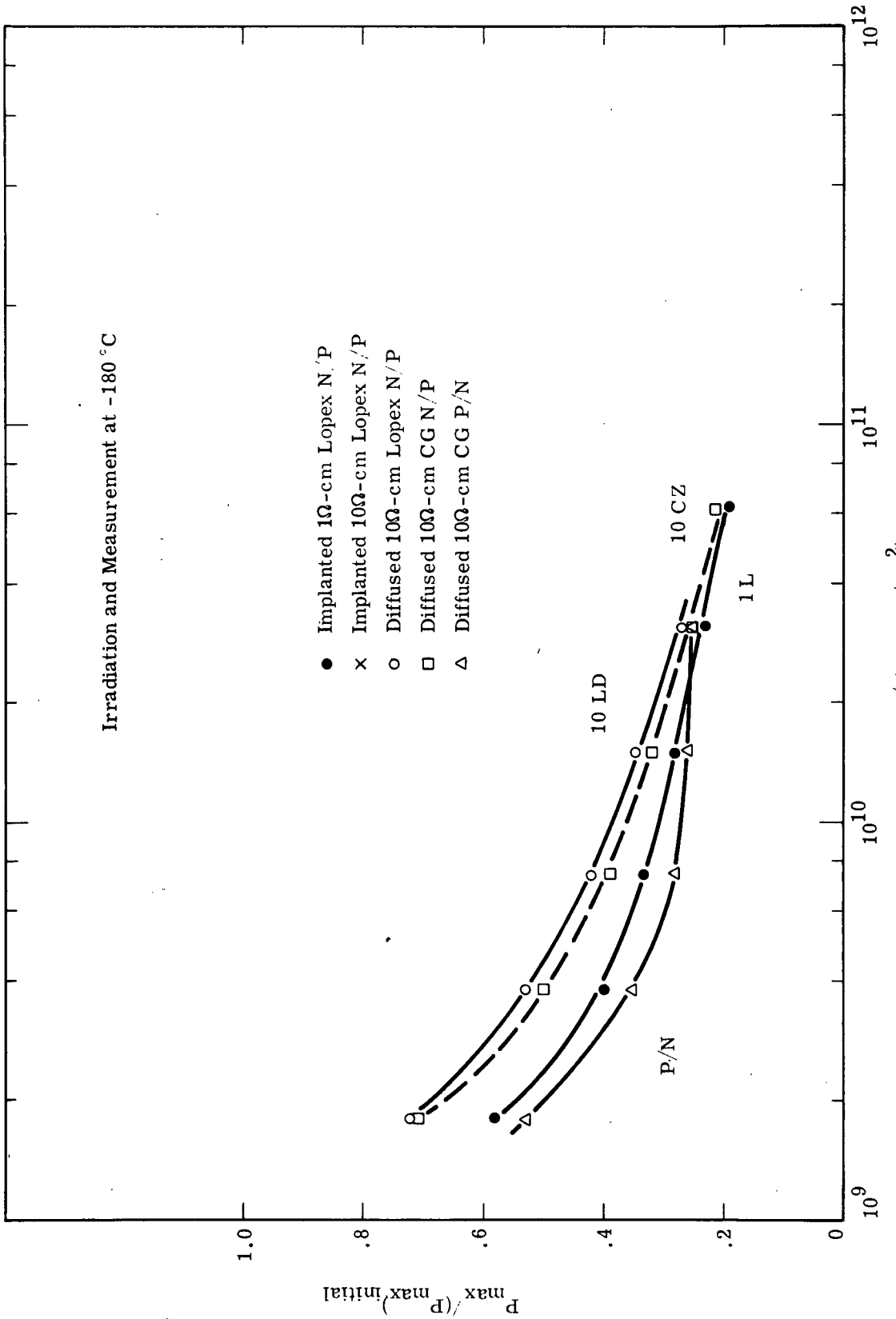

Figure 13. P_{max} Degradation at -180 °C.

1-6329

Table II. Critical 1 MeV Proton Fluences. ^{2}
All entries are x 10^{10} protons/cm^2.

A. Fluence for 25% Decrease in I_{sc}

Cell Type	Irradiation and Measurement Temperature			
	28 °C	-70 °C	-160 °C	-180 °C
Implanted 1Ω-cm Lopex N/P	2 x 10^{10}	-	0.3	0.1
Implanted 10Ω-cm Lopex N/P	5	1	0.4	-
Diffused 10Ω-cm Lopex N/P	10	0.5	0.3	0.2
Diffused 10Ω-cm CG N/P	8	-	0.3	0.2
Diffused 10Ω-cm CG P/N	1	-	0.3	0.1

B. Fluence for 50% Decrease in I_{sc}

Cell Type	Irradiation and Measurement Temperature			
	28 °C	-70 °C	-160 °C	-180 °C
Implanted 1Ω-cm Lopex N/P	11 x 10^{10}	2	0.9	0.3
Implanted 10Ω-cm Lopex N/P	23	4	2	-
Diffused 10Ω-cm Lopex N/P	40	3	0.7	0.7
Diffused 10Ω-cm CG N/P	28	3	0.8	0.7
Diffused 10Ω-cm CG P/N	4	1	1	0.4

C. Fluence for 25% Decrease in P_{max}

Cell Type	Irradiation and Measurement Temperature			
	28 °C	-70 °C	-160 °C	-180 °C
Implanted 1Ω-cm Lopex N/P	1 x 10^{10}	-	0.2	<0.1
Implanted 10Ω-cm Lopex N/P	3	0.7	0.4	-
Diffused 10Ω-cm Lopex N/P	6	0.4	0.2	0.2
Diffused 10Ω-cm CG N/P	5	-	0.3	0.2
Diffused 10Ω-cm CG P/N	0.9	-	0.3	-

Table II. Continued.

D. Fluence for 50% Decrease in P_{max}

Cell Type	Irradiation and Measurement Temperature			
	28 °C	-70 °C	-160 °C	-180 °C
Implanted 1Ω-cm Lopex N/P	6×10^{10}	2	0.6	0.3
Implanted 10Ω-cm Lopex N/P	14	3	2	-
Diffused 10Ω-cm Lopex N/P	24	2	0.6	0.5
Diffused 10Ω-cm CG N/P	21	2	0.6	0.4
Diffused 10Ω-cm CG P/N	2	~1	0.7	0.2

Table III. $(P_{max})/(P_{max})_{initial}$ versus Temperature After Fixed Temperature Irradiations.

Irradiation Condition	Cell Type	$(P_{max})/(P_{max})_{initial}$			
		28°C	-70°C	-160°C	-180°C
2.5×10^{11} p/cm^2 at 28 °C	Implanted 1Ω-cm Lopex N/P	.28	.22		.15
	Implanted 10Ω-cm Lopex N/P	.38	.34		.27
	Diffused 10Ω-cm Lopex N/P	.50	.41		.30
	Diffused 10Ω-cm CG N/P	.45	.38		.37
	Diffused 10Ω-cm CG P/N	.20	.22		.24
2.5×10^{11} p/cm^2 at -70 °C	Implanted 1Ω-cm Lopex N/P	.36	.23	.20	
	Implanted 10Ω-cm Lopex N/P	.41	.29	.23	
	Diffused 10Ω-cm Lopex N/P	.33	.25	.21	
	Diffused 10Ω-cm CG N/P	.38	.21	.18	
	Diffused 10Ω-cm CG P/N				
2.5×10^{11} p/cm^2 at -160 °C	Implanted 1Ω-cm Lopex N/P	.39	.30	.17	
	Implanted 10Ω-cm Lopex N/P	.51	.36	.21	
	Diffused 10Ω-cm Lopex N/P	.33	.25	.18	
	Diffused 10Ω-cm CG N/P	.29	.27	.19	
	Diffused 10Ω-cm CG P/N	.32	.31	.26	

degradation at a given measurement temperature is influenced by the irradiation temperature. However a trend common to all the cell types is not observed. For example, implanted 10 ohm-cm Lopex N/P cells showed degradation to 38% of initial 28 °C 5.8 mW/cm^2 maximum power when irradiated at 28 °C but only to 51% of initial 28 °C 5.8 mW/cm^2 maximum power when irradiated at -160 °C. Instead of showing greater fractional decrease under 28 °C irradiation, diffused 10 ohm-cm Lopex N/P cells degraded only to 50% of initial 28 °C 5.8 mW/cm^2 output under 28 °C irradiation but to 33% of initial when irradiated at -160 °C. It appears to be possible that after relatively high fluence irradiation levels, P/N cells and implanted N/P cells may show less and diffused N/P cells more output degradation at specific operating temperature as irradiation temperature decreases. Further investigation may be warranted in this area.

3.3.3. Annealing Effects

The fact that cell performance at a given temperature after irradiation is dependent upon temperature during irradiation indicates a temperature dependence to the formation or stability of the radiation-induced crystal defects. A possible distinct difference between the influence of the defects formed in diffused and ion implanted cells suggests complexity beyond that which could be investigated in this study. However a test was undertaken to determine whether other parameters associated with a mission environment might also influence degree of degradation of an irradiated cell.

A group of four N/P cells selected at random from available test lots were irradiated at -186 °C to 1.7 x 10^{11} protons/cm^2. After measurement the cells were held at -186 °C in the dark for 6 hours, under 5 mW/cm^2 3200 °K color temperature illumination for 5 hours then under 100 mW/cm^2 illumination for 6 hours. Finally the cells were warmed to 28 °C for 1 hour before returning them to -186 °C for final measurements. The separate ultrastable tungsten source used for cell measurements was carefully monitored to insure better than 1% reproducibility over this period. An example of the sequence of cell output measurements obtained is shown in Figure 14. It can be seen that modest but significant performance recovery of this implanted 10 ohm-cm Lopex cell

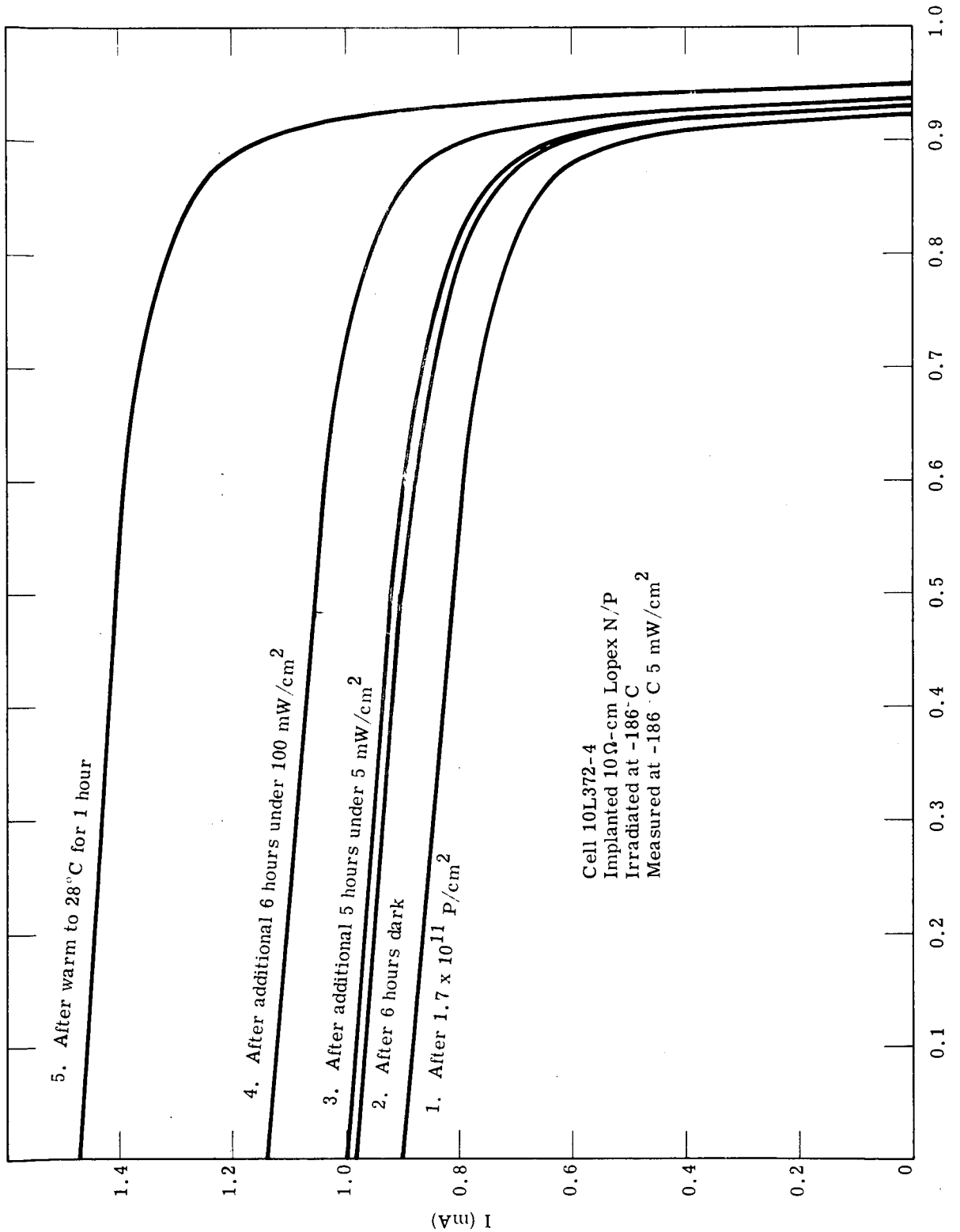

Figure 14. Variation of Output I-V Characteristic During In-Situ Storage.

occurred during 6 hours of dark storage at -186 °C and little additional recovery occurred during the next 5 hours under 5 mW/cm^2 illumination. Six hours under 100 mW/cm^2 illumination resulted in another step increase of output performance and then warm-up to room temperature raised -186 °C P_{max} output to nearly double the immediate post-irradiation level.

Normalized post-irradiation I_{sc} and P_{max} values for all four cells after each storage cycle are tabulated in Table IV. It is to be noted that while both of the implanted 10 ohm-cm Lopex cells showed some recovery under dark storage, neither of the other cells exhibited any improvement until after the 5 hour 5 mW/cm^2 storage. It is possible that the 'dark' anneal of the implanted 10 ohm-cm Lopex cells could actually have occurred during the 5 minute period the cells were illuminated for measurement purposes. A definite improvement occurred in all cells during storage under 100 mW/cm^2 illumination.

From Table IV it is obvious that greatest fractional recovery of cell performance produced by a temporary warm-up to room temperature. After completion of irradiation and measurement, all of the cells in the in-situ tests used to generate Figures 6 through 13 were allowed to warm up to room temperature overnight and were remeasured at low temperatures a final time the following day. In every case a performance improvement was observed. The improvement was generally largest for the lowest temperature irradiations and least but still significant in cells irradiated at 28 °C. Observed changes in P_{max} are given in Table V.

3.4 Effect of Irradiation on the Equivalent Circuit Model

Consideration of pre- and post-irradiation dark forward characteristics allows the influence of radiation damage on the individual components of the cell model to be determined. Figure 15 shows an example of 28 °C and -183 °C dark forward characteristics of a typical cell before and after irradiation at 28 °C. The 28 °C dark characteristic is substantially altered after irradiation but the -183 °C characteristic is modified only slightly and only at current levels exceeding a few milliamperes. This means that at room temperature there are

Table IV. Performance Data on Cells Stored at -186 °C
(After Irradiation to 1.7×10^{11} p/cm^2 at -186 °C)

Cell	Type	Test Condition -186 °C, 5 mW/cm^2	$(I_{sc})/(I_{sc})_{initial}$	$(P_{max})/(P_{max})_{initial}$
10L372-4	Implanted 10Ω-cm Lopex N/P	1. After Irradiation	0.23	0.17
		2. After 6 hrs. Dark	0.25	0.19
		3. After 5 hrs. 5 mW/cm^2	0.25	0.20
		4. After 6 hrs. 100 mW/cm^2	0.28	0.23
		5. After Warm-up to 28 °C	0.37	0.33
10L372-5	Implanted 10Ω-cm Lopex N/P	1. After Irradiation	0.25	0.18
		2. After 6 hrs. Dark	0.27	0.19
		3. After 5 hrs. 5 mW/cm^2	0.27	0.19
		4. After 6 hrs. 100 mW/cm^2	0.28	0.23
		5. After Warm-up to 28 °C	0.34	0.31
1L326-5	Implanted 1Ω-cm Lopex N/P	1. After Irradiation	0.15	0.10
		2. After 6 hrs. Dark	0.15	0.10
		3. After 5 hrs. 5 mW/cm^2	0.16	0.11
		4. After 6 hrs. 100 mW/cm^2	0.18	0.13
		5. After Warm-up to 28 °C	0.23	0.16
10CG84-9	Diffused 10Ω-cm N/P	1. After Irradiation	0.19	0.16
		2. After 6 hrs. Dark	0.19	0.16
		3. After 5 hrs. 5 mW/cm^2	0.21	0.18
		4. After 6 hrs. 100 mW/cm^2	0.23	0.20
		5. After Warm-up to 28 °C	0.27	0.25

Table V. Effect of 28 °C Anneal on P_{max} of Irradiated Cells.

Cell Type	$(P_{max})/(P_{max})_{initial}$ - After 2.5×10^{11} p/cm^2 and After Overnight at 28 °C			
	Irradiate -160 °C Measure -160 °C	Irradiate -70 °C Measure -160 °C	Irradiate -70 °C Measure -70 °C	Irradiate 28 °C Measure 28 °C
Implanted 1Ω-cm Lopex N/P	0.17 - 0.26	0.20 - 0.24	0.23 - 0.27	0.28 - 0.31
Implanted 10Ω-cm Lopex N/P	0.21 - 0.31	0.23 - 0.26	0.29 - 0.33	0.38 - 0.41
Diffused 10Ω-cm Lopex N/P	0.18 - 0.24	0.21 - 0.22	0.25 - 0.27	0.50 - 0.54
Diffused 10Ω-cm CG N/P	0.19 - 0.25	0.18 - 0.26	0.21 - 0.23	0.45 - 0.46
Diffused 10Ω-cm CG P/N	0.26 - 0.29			0.20 - 0.20

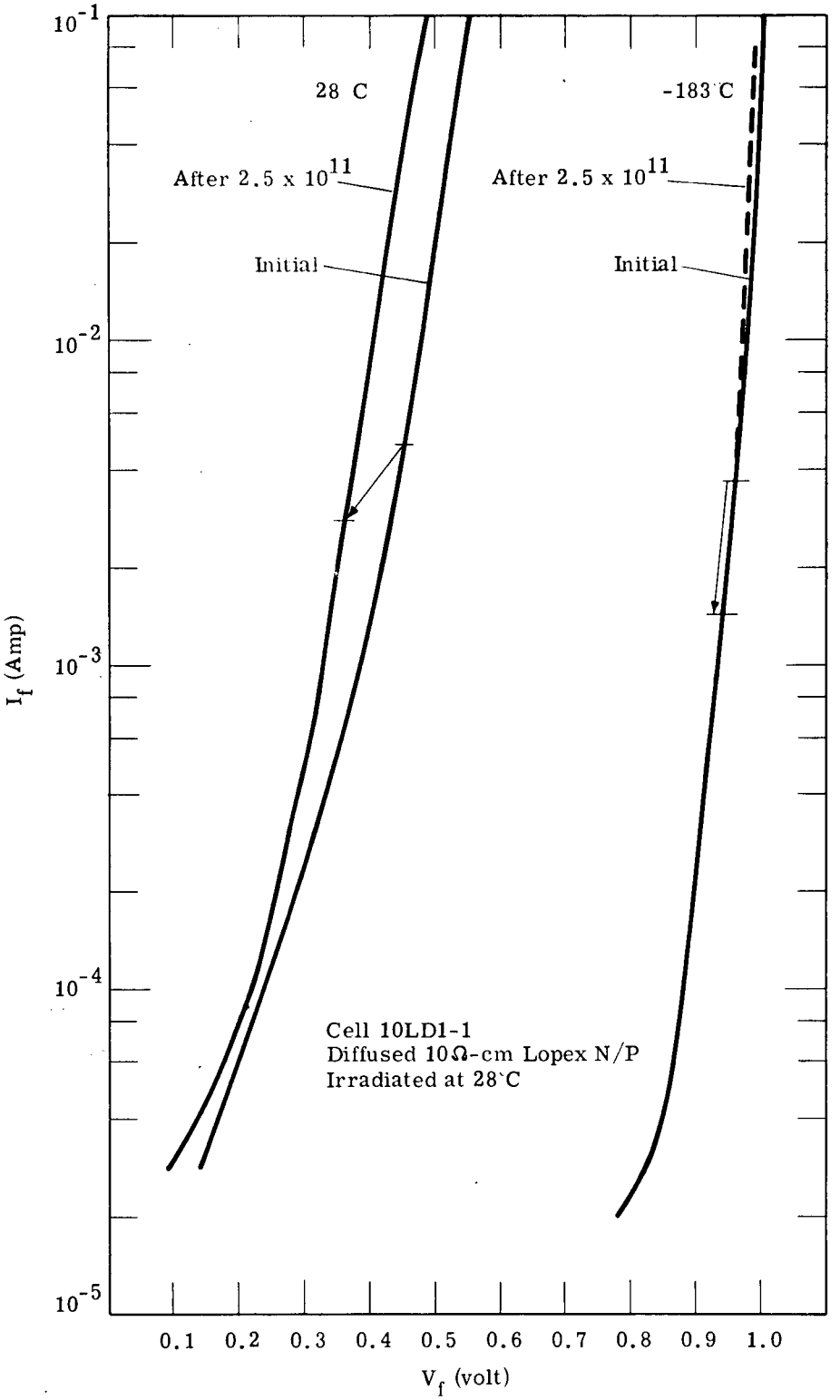

Figure 15. The Effect of Irradiation on the Dark I-V Characteristic.

1-6331

basically two components to the degradation: (1) minority carrier collection efficiency decreases because of increased recombination in the base, and (2) junction saturation current increases because of the formation of generation-recombination centers in the junction depletion region. Loss of collection efficiency appears as decrease in output current while increased junction saturation current results in a loss of output voltage. At low temperature and for low illumination intensities cell degradation is essentially entirely due to loss of collection efficiency.

The example cell of Figure 15 was experimentally observed to degrade at 28 °C from initial I_{sc} of 4.8 mA to 2.8 mA after irradiation and from 3.5 to 1.4 mA at -183 °C. From the forward curves it can be seen that a 90 mV loss of V_{oc} is expected at 28 °C while the -183 °C should be only 20 mV. These values were experimentally verified.

Cell edge currents are of major consequence at low temperatures. No changes in edge components have been observed. Consider Figure 16 which shows an example cell with a severe edge channel double slope problem at -184 °C. Pre- and post-irradiation illuminated characteristics for this cell were shown in Figure 4. The edge channel which has resistance of only 48 ohms and dominates the characteristic between its turn-on at 0.4 volt and turn-on of the cell junction just below 1 volt is observed to be totally unaffected by irradiation to 1.7×10^{11} p/cm^2 fluence.

The body component R_{JD} of junction shunt resistance in a good cell has no effect on the output I-V characteristics over the 28 °C and lower temperature range. It is possible that minor changes may occur in this component due to irradiation but they are of no operational consequence. Data taken during in-situ radiation tests did not resolve changes below 10^{-5} ampere associated with this component in a good cell.

The equivalent circuit model of the cell is repeated in Figure 17 to indicate radiation sensitivity of the circuit elements. A Schottky barrier in series with the p-n junction has been omitted because although such a barrier has previously been observed at low temperatures, its absence is now assured in a cell properly fabricated for low temperature operation. The effect of irradiation on this equivalent circuit model is basically the same as has been described by Stofel and Joslin.[8]

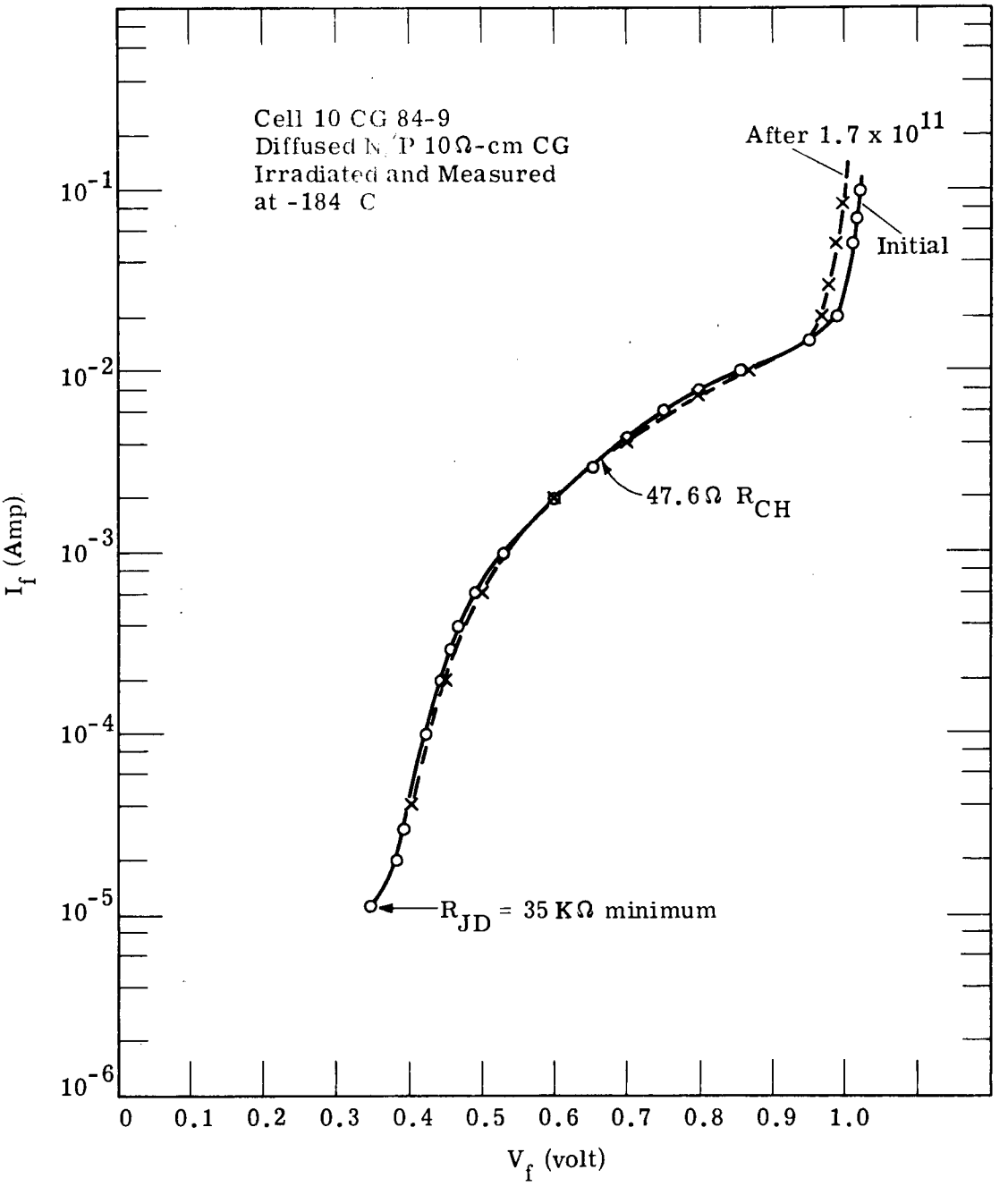

Figure 16. Dark I-V Characteristic of Excessive Edge Conduction Cell.

1-6332

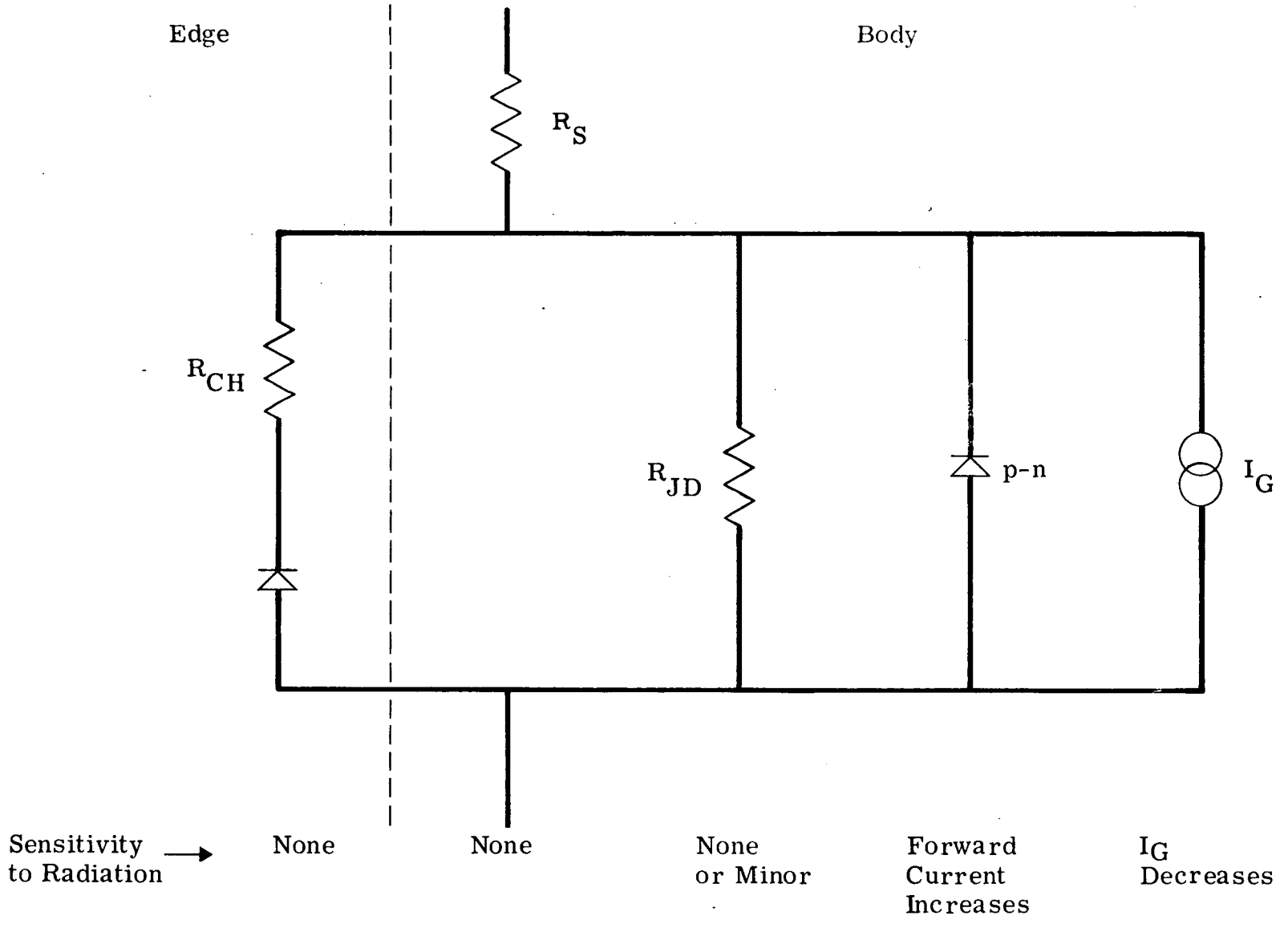

Figure 17. The Influence of Irradiation on the Solar Cell Equivalent Circuit Model.

SECTION 4
CELL SPECIFICATION

Specification of design parameters for a solar cell to be employed on a low temperature, low illumination intensity environment mission must be based upon minimization of potential operational deficiencies due to fabrication with simultaneous maximization of cell output and resistance to radiation-induced degradation. While such a specification can easily be made, many parameters must be selected almost arbitrarily and ultimate performance of even the optimum cell will be drastically reduced by exposure to a high energy proton radiation environment. Assuming that any solar cell being considered will not exhibit serious initial performance deficiencies under low temperature and intensity, true optimization can be approached by first considering the mode of utilization required.

It is clear that regardless of the detail of its design parameters, any silicon solar employed on a low temperature mission will be extremely vulnerable to radiation degradation. All cell types tested have shown similar very rapid degradation due to proton exposure at low temperatures. It has been predicted[4] that the radiation environment of Jupiter may include high fluxes of protons with sufficient energies to penetrate even coverglasses as thick as 100 mils. In this case serious performance degradation will be incurred.

Large area arrays with 100 mil or thicker covers are probably not a feasible approach to a solar cell power supply for a Jupiter flight. After compensation for possible radiation induced degradation, a cell area exceeding 4000 cm^2 per watt would be necessary for -140 °C, 1/26 solar constant illumination operation in the vicinity of Jupiter.

A more practical solution could involve the use of small heavily shielded cell arrays combined with solar concentrators to increase illumination intensity on the panel area. Solar concentrators are not used for Earth orbit applications because cell surface intensities greater than one solar constant

result in heating and series resistance problems with overall decrease in performance-weight-cost optimization. However at low temperature under 1/26 solar constant illumination, a concentration factor exceeding 10 could be employed without heating or series resistance problem. In this case a cell area of 150 cm^2 or less per watt could be sufficient. The small area array would be shielded with as much as 100 mils of silica coverplate to protect against protons with energies up to 22 MeV. As highest cell efficiency is achieved at lowest temperatures the cell array and its supports would be designed for maximum heat removal. A small panel/concentrator approach in addition to offering the possibility for adequately protecting the cells without excessive weight penalties would also provide a coincidental improvement in cell output. Minor shunt or double slope problems which might be significant at 1/26 solar constant become negligible at decade higher current levels.

4.1 Cell Specification

A cell optimized for use in a low temperature/low intensity environment can be similar to existing conventional cell structures. Provision must be made to assure absence of low temperature performance problems. The parameters below are recommended for cells to be utilized in a small panel/concentrator configuration with thick cover protection over cells. IPC considers these to define a best choice for the optimized cell. However, indicated parameters are not necessarily critical and as will be briefly discussed below, acceptable alternatives could be employed.

1.	Cell Structure:	N^+/PP^+
2.	Base Material:	Low oxygen/low dislocation
3.	Base Resistivity:	10 - 30 ohm-cm
4.	Cell Thickness:	8 - 10 mils
5.	Front Surface Finish:	Polish etched to mirror surface
6.	Junction Formation:	Diffusion or implantation

7.	Junction Depth:	0.3 - 0.5 micron
8.	Back surface P^+ Layer:	Alloyed aluminum
9.	Contact Material:	Aluminum or titanium-silver
10.	Front Contact Configuration*:	Standard 5 through 14 fingers plus contact bar. Up to 6% of active surface occupied.
11.	Series resistance*:	$\leq$ 0.3 ohms (2 x 2 cm cell)
12.	Shunt Resistance:	2000 ohms minimum
13.	Antireflective Coating:	CeO_2 or TiO_x applied before cell is sized
14.	Cell Surface Dimensions:	2 cm x 2 cm
15.	Method of Cell Sizing:	Scribing after contacting and AR coating
16.	Cover Protection*:	Glued fused silica as thick as possible up to 100 mils
17.	Interconnections:	Ultrasonically welded aluminum or soldered

Specification of an N^+/PP^+ cell structure is straightforward. P/N cells are considerably more sensitive to radiation damage at 28 °C than are N/P's and are definitely not superior to N/P's under low temperature irradiations. P/N's also show inferior performance at low temperature after being irradiated at room temperature and the choice of N/P follows. A back surface P^+ layer

*These recommendations apply specifically to the case of a heavily protected panel used in conjunction with a solar concentrator to increase intensity by a factor of approximately ten.

necessary to eliminate Schottky-barrier rectification effects at low temperature completes the N^+/PP^+ structure.

Investigations conducted elsewhere[2] have shown that cells made of crucible grown silicon exhibit greater loss of current with decreasing temperature than do cells made of low oxygen content material. As the crucible grown material cells do not exhibit any compensating improved performance or radiation resistance characteristics at low temperatures, choice of the low oxygen, low dislocation base material is also clear. Cells with 10 Ω-cm base resistivity showed slight overall radiation resistance superiority over 10 Ω-cm base cells. As at reduced temperatures there exists little dependence of cell V_{oc} on base resistivity the 1Ω-cm cells offers no advantageous initial performance. Optimum base resistivity is then at least 10 ohm-cm and could possibly be as high as 100 ohm-cm. In the absence of test data on 100 ohm-cm cells, specification not greatly above 10 ohm-cm is prudent.

Designation of cell thickness as 8 - 10 mils is somewhat arbitrary. Increasing cell thickness to more than twice the base minority carrier diffusion length results in negligible increase of output. At -140 °C a cell of 8 - 10 mils thickness should give maximum response.

The low temperature/intensity cell must have good junction characteristics. In order to insure low leakage it is possible to use a deep junction or a normally shallow junction with good uniformity characteristics. As a deep junction (~1 micron) results in noticeable loss of blue response, it is preferable to use a 0.3 to 0.5 micron junction introduced into a mirror finish surface without visible scratches or nonuniformities. The 0.3 to 0.5 micron depth is also somewhat deeper than normal but is required to give good results with aluminum contacts. A shallower 0.25 micron junction could be acceptable for titanium-silver contacts. Equally acceptable performance is observed with implanted and diffused junction cells.

The back surface P^+ layer below the contact metallization can be produced either by alloying aluminum into the silicon or by a deep diffusion. Alloyed aluminum is considered to be superior because it results in a layer

which is reflective to unabsorbed photons and consequently yields slight improvement in long wavelength response.

Optimized front contact configuration is dependent upon the method of cell utilization. A 2 x 2 cm cell operating under 1/26 solar constant illumination requires only a contact bar and perhaps two fingers to keep its series resistance to an acceptable level which does not have to be less than one ohm. However if a solar concentrator is used to increase cell surface illumination intensity to a level approaching one solar constant, contact configurations similar to those currently in use will be required. A 2 x 2 cm cell operating under 50 mW/cm^2 or greater illumination should have series resistance not greater than 0.3 ohm.

Antireflective coatings presently in use will be adequate for the low temperature cell. Choice of CeO_2 or TiO_x is made because of their better optical optimization for a covered cell but SiO_x is also acceptable. IPC considers it to be possible that the presence of antireflective coating over the cell edge could contribute to edge inversion effects and could increase the double slope edge conduction problem. No attempt has been made to investigate this possibility. If the cell is sized by scribing after contacts and AR coating are applied the probability of encountering an edge conduction problem is low.

Thickness of the cover protection is particularly important. In the absence of experimental data or reliable theory to characterize the trapped proton environment of Jupiter, it is recommended that 100 mils of fused silica be used to provide protection against energies up to 22 MeV. This recommendation should be modified by latest available information should design of a solar power supply actually be undertaken. It is also of considerable importance that equivalent thick protection be provided to the contact bar and cell back areas as well as to the active surface.

SECTION 5
TEST PLAN

Following fabrication of quantities of cells to be utilized on a low temperature/low intensity mission it would be necessary to eliminate any cells showing significant performance deficiencies. Observation of the dark forward I-V characteristic at -196 °C during direct submersion in liquid nitrogen will identify any cell with a Schottky-barrier contact problem, a low shunt resistance or a double slope problem. Only a low short-circuit current because of non-linear dependence of I_{sc} on temperature is not observed by this test. This non-linear current problem has not been associated with low oxygen content (Lopex) silicon cells but even for these types it would be desirable to make an illuminated measurement at -135 °C or -196 °C on a sample cell from each crystal used to confirm acceptable I_{sc}.

The simplified low temperature dark forward measurement is made using mechanical-electrical clip connections to the cell which is submerged into a dark liquid nitrogen bath. The forward I-V characteristic is displayed on a curve tracer oscilloscope. A linear display covering 0-10 mA and 0-1.2 volt is adequate. A good 2 x 2 cm cell will exhibit a characteristic similar to that in the upper display of Figure 18 meeting the following conditions:

(1) forward current < 0.5 mA at 0.90 volt

(2) forward current > 10 mA at 1.1 volt

A cell with low shunt resistance or double slope problem will violate requirement (1) while a cell with rectifying contact will not meet requirement (2).

A cell which passes the above acceptance test could still have low short circuit current at -135 °C. If the cell is fabricated from low oxygen float zone or Lopex type material, low I_{sc} is not expected. But because the mechanism for non-linear dependence of I_{sc} on temperature has not been determined it could be advisable to make a low temperature/low intensity output measurement on at least one sample cell from each silicon crystal lot. A single measurement

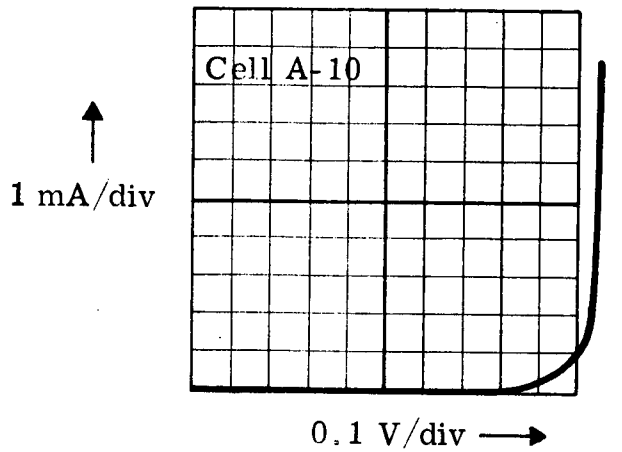

a. Typical Good Cell

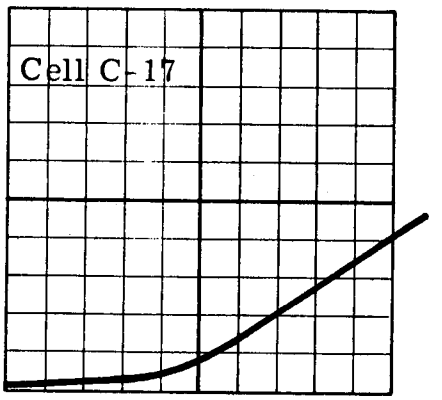

b. Cell with Non-Ohmic Rear Contact

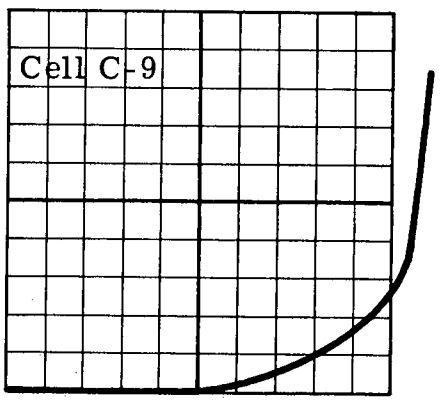

c. Cell with Excessive Conduction at 0.8 volt

Figure 18. Representative Dark Linear I-V Characteristics at 77 °K.

at -135 °C or -196 °C under low intensity AMO spectrum illumination should confirm acceptability of cells from the same crystal. An acceptable cell will test as follows:

Minimum I_{sc} 0.22 $(mA/cm^2)/(mW/cm^2)$ at -135 °C

Minimum I_{sc} 0.20 $(mA/cm^2)/(mW/cm^2)$ at -196 °C

SECTION 6

REFERENCES

1. Kirkpatrick, A. R., Ho, J. C. and Bartels, F. T. C., 'Analysis Report Volume I', Contract NAS2-5516.

2. Brandhorst, H. W. and Hart, R. E., 'Spectral Responce of Silicon Solar Cells at Low Temperatures', p. 142, Conference Record of Eighth IEEE Photovoltaic Specialists Conference, Seattle, August 1970.

3. Ho, J. C., Bartels, F. T. C. and Kirkpatrick, A. R., 'Solar Cell Low Temperature, Low Solar Intensity Operation', p. 150, Conference Record of Eighth IEEE Photovoltaic Specialists Conference, Seattle, August 1970.

4. Haffner, J. W., 'Calculated Dose Rates in Jupiter's Van Allen Belts', Paper 69-18, AIAA 7th Aerospace Sciences Meeting, New York, January 1969.

5. Haffner, J. W., 'Natural Nuclear Radiation Environments for the Grand Tour Missions', IEEE Trans. Nuc. Science, NS-18, No. 6, 443, December 1971.

6. Wilsey, N. D. and Lambert, R. J., 'Low Temperature Irradiations of Silicon Solar Cells with 1 MeV Electrons', p. 169, Conference Record of Eighth IEEE Photovoltaic Specialists Conference, Seattle, August 1970.

7. Debs, R. J. and Hanes, N. R., 'Preliminary Results of Radiation and Jupiter Environment Tests on Solar Cells', p. 155, Conference Record of Eighth IEEE Photovoltaic Specialists Conference, Seattle, August 1970.

8. Stofel, E. and Joslin, D., 'Low-Energy Proton Damage to Silicon Solar Cells', IEEE Trans. Nuc. Science, NS-17, No. 6, 250, December 1970.